PHYTOTHERAPY RESEARCH
Phytother. Res. **26**: 772–777 (2012)
Published online 24 November 2011 in Wiley Online Library
(wileyonlinelibrary.com) **DOI**: 10.1002/ptr.3621

Drug–drug Interactions between Ketoconazole and Berberine in Rats: Pharmacokinetic Effects Benefit Pharmacodynamic Synergism

Yanmi Zhou,[1†] Ping He,[2†] Aiming Liu,[3] Lixin Zhang,[4] Yunde Liu[2] and Renke Dai[1,3]*

[1]School of Life Science, University of Science and Technology of China, Hefei, Anhui 230026, China
[2]School of Medical Laboratory Science, Tianjin Medical University, Tianjin 300070, China
[3]Zhongshan PharmaSS Corporation, Zhongshan, Guangdong 528437, China
[4]Institute of Microbiology, Chinese Academy of Sciences, Beijing 100000, China

Ketoconazole (KTZ), a clinical antifungal agent, is a known inhibitor of CYP3A and permeability glycoprotein (P-gp). Berberine (BBR), a natural plant-derived product used for gastroenteritis, is a substrate of P-gp. Recently, a synergistic antifungal effect of KTZ combined with BBR has been revealed. In this study, we performed both *in vivo* and *in vitro* experiments to explore whether pharmacokinetic interactions between KTZ and BBR would benefit their phamacodynamic synergism. After oral co-administration of 10 mg/kg KTZ with 60 mg/kg BBR, the average area under the curve (AUC) and the maximum concentration (C_{max}) for KTZ increased to 215% and 449% ($p < 0.05$), respectively, in male rats and 157% and 172% ($p < 0.05$), respectively, in female rats, compared with those administered KTZ alone. Area under the curve and C_{max} for BBR increased to 173% and 142%, respectively, compared with those administered BBR alone. After intravenous co-administration of 0.5 mg/kg KTZ and 0.8 mg/kg BBR, the pharmacokinetic properties of KTZ remained the same, but AUC of BBR increased to 254% ($p < 0.05$) compared with those administered BBR alone. In rat liver microsomes, inhibitory concentration $(IC)_{50}$ of BBR inhibiting KTZ depletion was determined to be 103 μM. These resulting pharmacokinetic interactions may benefit their pharmacodynamic synergism to a certain extent. Copyright © 2011 John Wiley & Sons, Ltd.

Keywords: ketoconazole; berberine; pharmacokinetic; drug–drug interactions.

INTRODUCTION

Systemic fungal infections are increasingly becoming a serious problem in clinical practice. These infections are usually life-threatening, especially for the immunocompromised patients (Shao *et al*., 2007). Commonly prescribed antifungal agents can lead to high risks of nephrotoxicity and hepatotoxicity in clinic patients (Sabra and Branch, 1990; Garcia Rodriguez *et al*., 1999). The alarming increase in drug resistance is turning out to be another challenge. Combination therapy has been adopted as an approach to lower the dosage, lessening the adverse effects and reducing the incidence of drug-resistant strains (Gellen-Dautremer *et al*., 2010).

Ketoconazole (KTZ) is an imidazole derivative commonly prescribed for both superficial and systemic treatment of mycotic infections (Rodriguez and Acosta, 1997). However, a high dosage of KTZ can cause fatal hepatic necrosis, with its major metabolite *N*-deacetyl-KTZ playing an important role (Findor *et al*., 1998). A low amount of KTZ together with *Pelargonium graveolens* has been used for the treatment of trichophyton infections (Shin and Lim, 2004). A modest therapeutic advantage has also been found for KTZ when co-administered with amphotericin B, cyclosporin, estragole, xanthorrhizol and copiamycin (Graybill *et al*., 1980; Uno *et al*., 1983; Gerntholtz *et al*., 2004; Rukayadi *et al*., 2009).

* Correspondence to: Renke Dai, Zhongshan PharmaSS Corporation, National Health Technology Park, Zhongshan, Guangdong, 528437, China.
E-mail: renke_dai@yahoo.com
†Both authors contributed equally.

Berberine (BBR), a plant-derived isoquinoline alkaloid from the roots and bark of *Berberis aristata* or *Coptis chinensis*, has long been used as a treatment of gastroenteritis and secretory diarrhoea. Recently, the antifungal activity of BBR with low cytotoxicity to human cells has also been reported (Ficker *et al*., 2003; Mantena *et al*., 2006). Potent synergism against fluconazole-resistant *Candida albicans* using a combination of BBR and fluconazole has been reported (Iwazaki *et al*., 2010). Moreover, a synergistic antifungal effect has been confirmed using the combination of BBR and amphotericin B in an infectious mice model (Han and Lee, 2005). Recently, we have identified 12 potential combination therapies synergizing with low-dosage KTZ for antifungal activity, where BBR has been identified as the second most potent (Zhang *et al*., 2007).

In this study, we conducted *in vivo* and *in vitro* experiments to explore whether pharmacokinetic interactions between KTZ and BBR existed and whether an increase in their exposure level was beneficial to their pharmacodynamic synergism.

MATERIALS AND METHODS

Chemicals and reagents. BBR, phenacetin and KTZ, purity > 98.0%, were obtained from the National Institute for the Control of Pharmaceutical and Biological Products (NICPBP; Beijing, China). Propranolol was purchased from Sigma–Aldrich (St Louis, MO, USA). Nicotinamide adenine dinucleotide phosphate hydrogen (NADPH) was acquired from BD Gentest (Woburn, MA, USA). Acetonitrile (ACN) and methanol of high

Received 11 February 2011
Revised 21 June 2011
Accepted 25 June 2011

performance liquid chromatography (HPLC) grade were purchased from Dikma (DIKMA Technology, Inc., USA). Deionized water was produced using a Milli-Q system (Millipore, Milford, MA, USA).

Animals. Specific-pathogen-free Sprague-Dawley rats (6–8 weeks old, 200 ± 20 g) were purchased from the laboratory animal services center of Southern Medical University in China. They were kept under constant temperature (23 ± 2 °C) and a standard 12-h dark–light cycles with humane care. All the rats were acclimatized to animal facilities for at least 1 week with free access to food and water. Before experiments, the rats were deprived of food but given free access to water overnight. The animal protocols for experiments were performed in accordance with Public Health Service policies, the Animal Welfare Act, and approved by The Laboratory Animal Committee of Guangzhou Institute of Biomedicine and Health, Chinese Academy of Sciences.

In vivo pharmacokinetic interactions between BBR and KTZ.

Oral administration. Ketoconazole (10 mg/kg) and BBR (60 mg/kg) were dissolved in boiling physiological saline acidified with 5% (v/v) HCl. The mixture was cooled to room temperature and then adjusted to pH 7.0 before administration. About 0.2 mL blood was collected from the choroid vein at time zero before injection and subsequently at 0.083, 0.25, 0.5, 0.75, 1.0, 1.5, 3, 4, 6, 8, 12, 18, 24, 30 and 36 h after administration. Samples were transferred immediately into heparinized tubes and centrifuged at 6000 × **g** for 9 min under 4 °C to separate the plasma. Finally, all the plasma samples collected were stored at −80°C until analysis.

Intravenous administration. Ketoconazole and BBR were dissolved in ethanol first, diluted 100-fold by boiling physiological saline acidified with 5% (v/v) HCl. The mixture was cooled to room temperature and then adjusted to pH 7.0 before intravenous administration. Ketoconazole (0.5 mg/kg) and BBR (0.8 mg/kg) were administered discretely through the femoral vein as controls, or KTZ (0.5 mg/kg) was injected along with 0.8, 4 and 20 mg/kg BBR to evaluate the potential pharmacokinetic interaction. Blood samples were collected from the choroid vein at time zero before injection and subsequently at 0.03, 0.13, 0.33, 0.67, 1.5, 3, 5, 8, 12, 16, 24 and 36 h after administration. Samples were transferred immediately into heparinized tubes and centrifuged at 6,000 × **g** and 4 °C for 9 min to separate the plasma. Finally, all the plasma samples collected were stored at −80°C until analysis.

Inhibitory effect of BBR on the depletion of KTZ.

Preparation of rat liver microsomes. Pooled rat liver microsomes (RLM) were prepared according to a previous report (Hutson and Higgins, 1987). Briefly, 20 livers of Sprague-Dawley rats (10 female and 10 male) were dissected after perfusion and homogenization. The resulting solutions were centrifuged twice at 9000 × **g** for 20 min. Microsomes were isolated by centrifugation at 100000 × **g** for 60 min. The precipitation was reconstituted in phosphate buffer and stored at −80°C until use. The protein concentration of microsomes was determined using Lowry assay (Lowry *et al*., 1951).

Determination of the kinetic parameter K_m of KTZ. Ketoconazole (0.02, 0.05, 0.2, 1 and 5 μM) was incubated with RLM (0.3 mg/mL) diluted in 0.1 M phosphate buffer (pH 7.4, EDTA 1 mM) for 5 min at 37 °C. The final concentration of organic solvent did not exceed 0.5%. Reactions were initiated by adding NADPH with a final concentration of 1 mM. Aliquots (0.1 mL) were removed to 0.2 mL of ice-cold acetonitrile containing internal standard (IS) to terminate the reaction at 0, 3, 6, 10, 15 and 20 min. The apparent Michaelis constant K_m was determined by the substrate depletion approach. The percentage of the remaining substrate versus time was fitted to first-order decay to calculate the apparent rate constant of substrate depletion (K_{dep}). The value of K_m was determined by fitting K_{dep} and substrate concentration [*S*] to Equation 1 proposed by Obach and Reed-Hagen (2002; cited in Nath and Atkins, 2006) using the Origin software (version 7.5, MicroCal Software, Inc., Northampton, MA).

$$K_{dep} = K_{dep}([s] \to 0) \times \left(1 - \frac{[S]}{[S] + K_m}\right) \qquad (1)$$

Apparent IC_{50} value of BBR for the depletion of KTZ. Various concentrations of BBR (0, 20, 50, 100, 200, 300, 400 and 500 μM) together with 0.05 μM KTZ (approximately its apparent K_m values as determined) were incubated in RLM. The incubation condition followed that above, after pre-incubation for 5 min at 37 °C; reactions were initiated by adding NADPH with a final concentration of 1 mM. Aliquots (0.1 mL) were removed to 0.2 mL of ice-cold acetonitrile containing IS to terminate the reaction at 20 min. The IC_{50} value (i.e., the BBR concentration that decreased the metabolic activity of KTZ by 50%) was determined by the non-linear regression of sigmoidal dose–response curves using Grafit 5.0.

Sample preparation. The plasma samples as well as *in vitro* samples were extracted by protein precipitation. Plasma samples were thawed at air temperature and vortexed for 2 min. Plasma samples (100 μL) and propranolol (20 μL) in ACN were added to a disposable tube. The mixture was vortexed slightly for 30 s. Then, 300 μL ACN was added to the tube and vortexed for 15 min. The well-vortexed plasma samples and *in vitro* samples were centrifuged at 17000 × **g** for 30 min. The up-layers were transferred to a new tube and centrifuged at 17000 × **g** for another 30 min. The supernatant was transferred to an HPLC autosampler and an aliquot of 20 μL was injected into the liquid chromatography-tandem mass spectrometry (LC–MS/MS) system.

LC-MS/MS assay.

Instruments and condition. Quantification of samples was performed using a LC-MS/MS system consisting of a Shimadzu LC-20 AD HPLC apparatus (Shimadzu, Japan) and Biosystems API 3000 triple-quadrupole mass spectrometer (Foster City, CA, USA) with an electrospray ionization source. A solvent A of H_2O:ACN (95:5, v/v) containing 10 mM ammonium acetate and a solvent B of H_2O:ACN (5:95, v/v) containing 10 mM ammonium acetate were used in all the gradient analysis. The gradient programme started with 15% solvent B for 0.3 min and then increased linearly to 100% solvent B within 0.2 min, held for 2.8 min and then dropped to 15% solvent B within 0.2 min, eventually equilibrated for 2.5 min.

Mass spectrometric conditions were optimized and performed using multiple reactions monitoring scan in

positive mode. The *m*/*z* transitions were set as 336.1/321.1 for BBR, 531.1/489.2 for KTZ and 260.10/116.2 for propranolol (IS).

Method validation. The assay was validated according to the *Food and Drug Administration Guidance on Bioanalytical Medical Method Validation* published in May 2001 as follows (US Food and Drug Administration, 2001). Selectivity was performed by analysing the blank plasma from six different sources to detect interference at the retention times of the analyte and IS. Linearity was determined by plotting the peak area ratios of analyte and IS against the concentrations of analyte in plasma in duplicate on three consecutive days. Inter- and intraday accuracy and precision were determined using three levels of quality control (QC) run on three validation days. On each day, six replicates were analysed together with an independently prepared calibration curve. Recovery of analyte was evaluated by comparing the mean peak areas of the regularly prepared QC samples ($n = 6$) with the mean peak areas of spiked-after extraction samples, representing the 100% recovery value. Stability of analyte was evaluated at different conditions. The spiked plasma samples were analysed after storage at room temperature for 4 h, at −20°C for 24 h, at −80°C for 1 month, and after three freeze–thaw cycles from −20°C to room temperature. The autosampler stability of analyte in rat plasma was evaluated by reinjecting the previously injected QC samples after a period of storage in the autosampler. The suitability of study samples being diluted with drug-free rat plasma (three times) on the day of assay was evaluated. The matrix effect was evaluated at two concentrations.

Data analysis. LC-MS/MS data acquisition and calibration were performed with Analyst 1.4.2 software (MDS Sciex, Canada). The pharmacokinetic parameters were calculated using the Drug and Statistics (DAS) version 2.0 software package (Anhui Provincial Center for Drug Clinical Evaluation, China). Data are expressed as mean ± SE. The independent-sample *t*-test was applied for the comparison of pharmacokinetic parameters of each group, the significance level set as $p < 0.05$.

RESULTS

LC-MS/MS method validation

A sensitive LC-MS/MS method has been developed and validated for simultaneous quantification of BBR and KTZ in rat plasma. Calibration curves were linear over the concentration range of 0.05–600 ng/mL for BBR and 0.4–6000 ng mL for KTZ, respectively, with correlation coefficients above 0.995. The relative standard deviation for inter- and intraday precision values was within 12.2% and relative error for accuracy ranged from −6.5% to 8.5%. The extraction recovery was on average 61.5 ± 8.6% for BBR and 99.8 ± 7.0% for KTZ. No significant degradation of BBR or KTZ was observed during sample storage, preparation and analysis period.

Effect of BBR on the pharmacokinetics of KTZ

The pharmacokinetic profile of KTZ either in treatment with KTZ alone or together with BBR showed a significant gender difference in rats (Fig. 1, Tables 1 and 2),

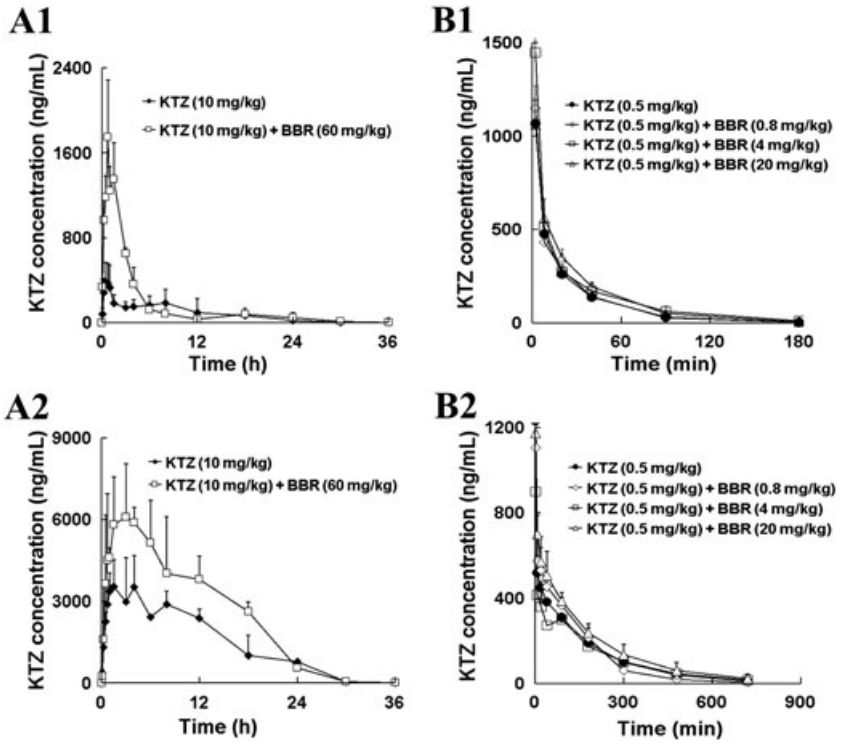

Figure 1. Serum KTZ concentration–time profiles in (A) oral administration and (B) i.v. administration. Each point and bar represents the mean and S.E. of six rats. (A1) Serum KTZ concentration–time profiles in male rats after oral administration of 10 mg/kg with or without 60 mg/kg BBR. (A2) Serum KTZ concentration–time profiles in female rats after oral administration of 10 mg/kg with or without 60 mg/kg BBR. (B1) Serum KTZ concentration–time profiles in male rats after i.v. administration of 0.5 mg/kg with 0, 0.8, 4 and 20 mg/kg BBR. (B2) Serum KTZ concentration–time profiles in female rats after i.v. administration of 0.5 mg/kg with 0, 0.8, 4 and 20 mg/kg BBR. KTZ: ketoconazole; BBR: berberine.

Table 1. Pharmacokinetic parameters (mean ± SE) of KTZ with or without administration of BBR in male rats ($n = 6$)

	KTZ (10 mg/kg), oral		KTZ (0.5 mg/kg), i.v.			
Parameters	–	BBR (60 mg/kg)	–	BBR (0.8 mg/kg)	BBR (4 mg/kg)	BBR (20 mg/kg)
AUC (μg/L/h)	2743 ± 1769	5890 ± 1160	351 ± 28	413 ± 134	454 ± 50**	447 ± 34**
$T_{1/2}$ (h)	3 ± 1	3 ± 1	0.43 ± 0.05	0.44 ± 0.03	0.61 ± 0.09**	0.5 ± 0.1
T_{max} (h)	0.6 ± 0.1	1 ± 0	–	–	–	–
CL (L/h/kg)	5 ± 2	1.8 ± 0.3	1.4 ± 0.1	1.3 ± 0.3	1.1 ± 0.1**	1.12 ± 0.09**
C_{max} (μg/L)	388 ± 188	1746 ± 540*	–	–	–	–

KTZ: ketoconazole; BBR: berberine; AUC: area under the blood concentration versus time curve; C_{max}: maximum concentration; $T_{1/2}$: half-life; T_{max}: time to C_{max}; CL: apparent plasma clearance.
*$p < 0.05$.
**$p < 0.01$ compared with those administered KTZ alone.

Table 2. Pharmacokinetic parameters (mean ± SE) of KTZ with or without administration of BBR in female rats ($n = 6$)

	KTZ (10 mg/kg), oral		KTZ (0.5 mg/kg), i.v.			
Parameters	–	BBR (60 mg/kg)	–	BBR (0.8 mg/kg)	BBR (4 mg/kg)	BBR (20 mg/kg)
AUC(μg/L/h)	54820 ± 13473	86059 ± 23290	1544 ± 123	1618 ± 188	1463 ± 426	2065 ± 292**
$T_{1/2}$ (h)	2.1 ± 0.4	3 ± 1	2.1 ± 0.4	1.7 ± 0.2	2.0 ± 0.2	1.7 ± 0.2*
T_{max} (h)	3 ± 1	4 ± 2	–	–	–	–
CL (L/h/kg)	0.19 ± 0.05	0.12 ± 0.03	0.33 ± 0.03	0.31 ± 0.04	04 ± 0.1	0.25 ± 0.04**
C_{max} (μg/L)	4060 ± 1139	7000 ± 1293*	–	–	–	–

KTZ: ketoconazole; BBR: berberine; AUC: area under the blood concentration versus time curve; C_{max}: maximum concentration; $T_{1/2}$: half-life; T_{max}: time to C_{max}; CL: apparent plasma clearance.
*$p < 0.05$.
**$p < 0.01$ compared with those administered KTZ alone.

similar to that previously reported (Huang *et al*., 2007). The maximum concentration (C_{max}), and area under the blood concentration versus time curve (AUC) were measured to be 388 ± 188 ng/mL and 2743 ± 1769 ng·h/mL, respectively, in male rats versus 4060 ± 1139 ng/mL and 54820 ± 13472 ng·h/mL, respectively, in female rats after oral administration of 10 mg/kg KTZ. Similarly, after intravenous administration of 0.5 mg/kg KTZ, the AUC, apparent plasma clearance (CL), and half-life ($T_{1/2}$)were determined as 351 ± 28 ng·h/mL, 1.4 ± 0.1 L/h/kg, and 0.43 ± 0.05 h, respectively, in male rats versus 1544 ± 123 ng·h/mL, 0.33 ± 0.03 L/h/kg, and 2.1 ± 0.4 h, respectively, in female rats.

The mean KTZ blood concentrations versus time profiles after oral and intravenous administration are shown in Fig. 1, and the pharmacokinetic parameters were determined and shown in Tables 1 and 2. After the co-administration of KTZ and BBR, AUC of KTZ increased to 215% in male rats and 157% in female rats compared with those administered KTZ alone. The value of C_{max} significantly increased by 349% ($p < 0.05$, 1746 ± 540 versus 388 ± 188 μg/L) in male rats and 72% ($p < 0.05$) in female rats compared with those administered KTZ alone. The effect of BBR on the pharmacokinetics of KTZ after intravenous administration seems to be dose dependent and gender related. Co-administration with a low dosage of 0.8 mg/kg BBR did not alter the pharmacokinetic profile of KTZ in both male and female rats. After co-administration with BBR 4 mg/kg, the pharmacokinetic parameters were significantly altered ($p < 0.01$) in male rats. In contrast, the KTZ pharmacokinetic profiles in female rats were not significantly altered. When 20 mg/kg BBR was co-administered, the exposures were slightly increased.

Effect of KTZ on the pharmacokinetics of BBR

Mean BBR blood concentrations versus time profiles after oral and intravenous administration are shown in Fig. 2, and the pharmacokinetic parameters are displayed in Table 3. Comparing the oral co-administration of BBR and KTZ with administration of BBR alone, the AUC of BBR increased by 73% with prolonged $T_{1/2}$ (11.60 ± 7.78 h versus 15.67 ± 7.73 h) and shortened time to C_{max} (T_{max}). The mean C_{max} increased by 42%. After intravenous co-administration with KTZ, the mean AUC of BBR increased by 154% with prolonged $T_{1/2}$ of 221% ($p < 0.05$) and lowered CL (6.76 ± 0.94 h versus 4.11 ± 2.63 L/h/kg).

Inhibition of KTZ metabolism

The depletion profiles of KTZ in RLM are plotted in Fig. 3A. The apparent enzyme kinetic parameter of K_m was calculated to be 0.049 μM. To determine the IC_{50} value, the concentration of KTZ was fixed at 0.05 μM, approximately the apparent K_m value; various concentrations of BBR were used to determine the inhibitory IC_{50}. The inhibitory profile is shown in Fig. 3B. The IC_{50} value was calculated to be 103 μM, indicating that BBR is not a potent inhibitor for the depletion of KTZ. In contrast, the apparent clearance of BBR in RLM was very slow (data not shown), thus the

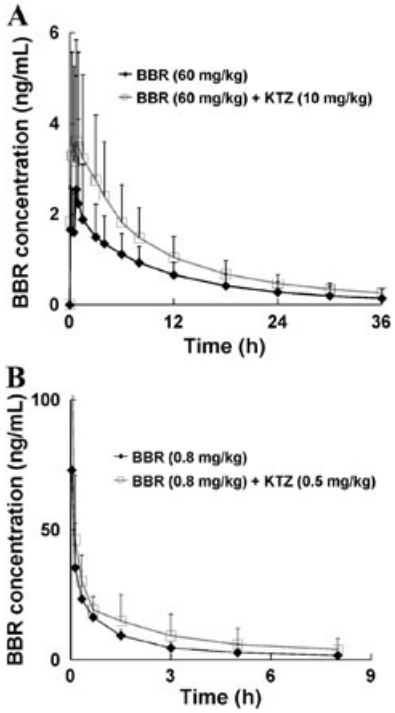

Figure 2. Serum BBR concentration–time profiles in rats. Each point and bar represents the mean and SE of six rats. (A) Oral administration of 60 mg/kg BBR with or without 10 mg/kg KTZ. (B) Intravenous administration of 0.8 mg/kg BBR with or without 0.5 mg/kg KTZ. KTZ: ketoconazole; BBR: berberine.

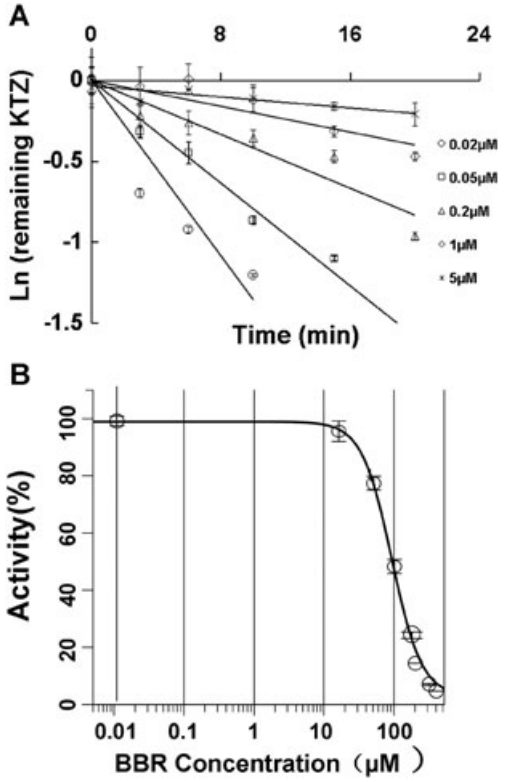

Figure 3. Elimination rate constants versus time profiles of KTZ and inhibitory effect of BBR on apparent depletion of KTZ in RLM. Each point and bar represents the mean and SE of six samples. (A) Elimination rate constants versus time profiles of KTZ in RLM. (B) Inhibitory profile of BBR on depletion of KTZ in RLM fitted by software of Grafit 5. KTZ: ketoconazole; BBR: berberine.

measurement to determine the IC_{50} of KTZ inhibiting BBR metabolism in RLM was not carried out.

DISCUSSION

Among the factors regulating the pharmacokinetic interactions, P-gp-mediated absorption and CYP3A-mediated metabolism are considered particularly important. P-gp is a membrane-bound glycoprotein mostly expressed in the intestine and commonly acts as an absorption barrier by transporting compounds from enterocytes to the intestinal lumen. Inhibition of P-gp results in increased absorption from the intestinal lumen into enterocytes and reduced elimination by excretion and/or secretion. CYP3A is the most important subfamily among the CYPs in human liver and small intestine. It catalyses the biotransformation of about half the available drugs (Guengerich, 1995). Inhibition of hepatic or gastrointestinal CYP3A results in a decrease in systemic metabolism and/or increase in absorption, leading to a higher exposure level.

In the present study, gender difference in the pharmacokinetic exposures of KTZ was observed after both oral and intravenous administrations. The AUC was lower in male rats than in female rats (Tables 1 and 2). The AUC of KTZ increased 2.2-fold in male rats and 1.6-fold in female rats after oral co-administration of KTZ with BBR, indicating that BBR regulates the pharmacokinetic properties of KTZ through absorption and/or elimination. However, the low dosage of BBR could not significantly modify KTZ exposure after intravenous co-administration. These data suggest that the inhibition of absorption in the intestine, instead of hepatic elimination, may play the main role in the pharmacokinetic interactions between KTZ and

Table 3. Pharmacokinetic parameters (mean ± SE) of BBR with or without administration of KTZ in rats ($n = 6$)

	BBR (60 mg/kg), oral		BBR (0.8 mg/kg), i.v.	
Parameters	–	KTZ (10 mg/kg)	–	KTZ (0.5 mg/kg)
AUC (μg/L/h)	26 ± 12	45 ± 17	75 ± 11	191 ± 150*
$T_{1/2}$ (h)	12 ± 7	16 ± 8	3.1 ± 0.9	10 ± 8*
T_{max} (h)	2.00 ± 1	1.4 ± 0.9	–	–
CL (L/h/kg)	482 ± 260	264 ± 127	6.8 ± 0.9	4 ± 2*
C_{max} (μg/L)	4 ± 2	6 ± 2	–	–

KTZ: ketoconazole; BBR: berberine; AUC: area under the blood concentration versus time curve; C_{max}: maximum concentration; $T_{1/2}$: half-life; T_{max}: time to C_{max}; CL: apparent plasma clearance.
*$p < 0.05$.

BBR. Berberine is both a substrate and an inhibitor of P-gp (Qiu *et al*., 2009); thus, the high concentration of BBR in the gastrointestinal tract may promote the absorption of KTZ by inhibiting the P-gp efflux activity for KTZ.

N-Deacetyl-KTZ is the primary metabolite of KTZ and is further metabolized by flavin-containing monooxygenases (FMO). In the present study, gender-related pharmacokinetic difference of KTZ was observed after both oral and intravenous administrations. The AUC in male rats was lower than that in female rats. This is consistent with a previous finding, where the elimination activity of KTZ is much higher in male rats than in female rats (Huang *et al*., 2007). The major initial metabolite of KTZ was further metabolized by FMO, and the activity of FMO was higher in male rats than in female rats (Rodriguez *et al*., 1999).

The AUC of BBR increased by 73% after oral co-administration with KTZ and 154% ($p < 0.05$) after intravenous co-administration. Ketoconazole is a potent inhibitor of P-gp and CYP3A. Berberine, a P-gp substrate, undergoes extensive first-pass metabolism by multiple P450s after oral administration (Liu *et al*., 2009). The responsible enzyme for BBR metabolism has not been identified, but it probably includes CYP3A. Thus, KTZ may reduce the BBR efflux by P-gp at the small intestine and inhibit the systemic elimination of BBR by hepatic or gastrointestinal CYP3A. Thus, AUC of BBR was slightly increased after intravenous or oral co-administration with KTZ.

In conclusion, pharmacokinetic drug interactions between KTZ and BBR were found to some extent in this study. The drug interactions may be mediated by the inhibition of intestinal P-gp, as intravenous administration displayed similar exposures between co-administrations and administrations alone. As BBR is a natural plant product widely used in East Asia, its pharmacodynamic synergism with KTZ may be beneficial for the development of a new treatment that can fight drug-resistant fungi.

Acknowledgments

This study was supported in part by Chinese government grants (2008AA02Z314, 2009DFA31530, and 2009ZX09301-015), Zhejiang Provincial Natural Science Foundation of China (grant Y2110016), and Ningbo Natural Science Foundation (grant 2011A610059).

Conflict of Interest

There are no potential conflicts.

REFERENCES

Ficker CE, Arnason JT, Vindas PS *et al*. 2003. Inhibition of human pathogenic fungi by ethnobotanically selected plant extracts. *Mycoses* **46**: 29–37.

Findor JA, Sorda JA, Igartua EB, Avagnina A. 1998. Ketoconazole-induced liver damage. *Medicina (B Aires)* **58**: 277–281.

Garcia Rodriguez LA, Duque A, Castellsague J, Perez-Gutthann S, Stricker BH. 1999. A cohort study on the risk of acute liver injury among users of ketoconazole and other antifungal drugs. *Br J Clin Pharmacol* **48**: 847–852.

Gellen-Dautremer J, Lanternier F, Dannaoui E, Lortholary O. 2010. Antifungal combination therapy in invasive fungal infections. *Rev Med Interne* **31**: 72–81. [In French.]

Gerntholtz T, Pascoe MD, Botha JF, Halkett J, Kahn D. 2004. The use of a cyclosporin-ketoconazole combination: making renal transplantation affordable in developing countries. *Eur J Clin Pharmacol* **60**: 143–148.

Graybill JR, Williams DM, Van Cutsem E, Drutz DJ. 1980. Combination therapy of experimental histoplasmosis and cryptococcosis with amphotericin B and ketoconazole. *Rev Infect Dis* **2**: 551–558.

Guengerich FP. 1995. Cytochrome P450 proteins and potential utilization in biodegradation. *Environ Health Perspect* **103** (Suppl 5): 25–28.

Han Y, Lee JH. 2005. Berberine synergy with amphotericin B against disseminated candidiasis in mice. *Biol Pharm Bull* **28**: 541–544.

Huang Q, Wang GJ, Sun JG, Hu XL, Lu YH, Zhang Q. 2007. Simultaneous determination of docetaxel and ketoconazole in rat plasma by liquid chromatography/electrospray ionization tandem mass spectrometry. *Rapid Commun Mass Spectrom* **21**: 1009–1018.

Hutson JL, Higgins JA. 1987. Reversible activation inactivation of the deacylation acylation cycle in rat-liver mivrosomes. *Biosci Rep* **7**: 73–80.

Iwazaki RS, Endo EH, Ueda-Nakamura T, Nakamura CV, Garcia LB, Filho BP. 2010. *In vitro* antifungal activity of the berberine and its synergism with fluconazole. *Antonie Van Leeuwenhoek* **97**: 201–205.

Liu Y, Hao H, Xie H, Lv H, Liu C, Wang G. 2009. Oxidative demethylenation and subsequent glucuronidation are the major metabolic pathways of berberine in rats. *J Pharm Sci* **98**: 4391–4401.

Lowry OH, Rosebrough NJ, Farr AL, Randall RJ. 1951. Protein measurement with the folin phenol reagent. *J Biol Chem* **193**: 265–275.

Mantena SK, Sharma SD, Katiyar SK. 2006. Berberine, a natural product, induces G1-phase cell cycle arrest and caspase-3-dependent apoptosis in human prostate carcinoma cells. *Mol Cancer Ther* **5**: 296–308.

Nath A, Atkins WM. 2006. A theoretical validation of the substrate depletion approach to determining kinetic parameters. *Drug Metab Dispos* **34**: 1433–1435.

Qiu W, Jiang XH, Liu CX, Ju Y, Jin JX. 2009. Effect of berberine on the pharmacokinetics of substrates of CYP3A and P-gp. *Phytother Res* **23**: 1553–1558.

Rodriguez RJ, Acosta D, Jr. 1997. N-deacetyl ketoconazole-induced hepatotoxicity in a primary culture system of rat hepatocytes. *Toxicology* **117**: 123–131.

Rodriguez RJ, Proteau PJ, Marquez BL, Hetherington CL, Buckholz CJ, O'Connell KL. 1999. Flavin-containing monooxygenase-mediated metabolism of N-deacetyl ketoconazole by rat hepatic microsomes. *Drug Metab Dispos* **27**: 880–886.

Rukayadi Y, Lee K, Lee MS, Yong D, Hwang JK. 2009. Synergistic anticandidal activity of xanthorrhizol in combination with ketoconazole or amphotericin B. *FEMS Yeast Res* **9**: 1302–1311.

Sabra R, Branch RA. 1990. Amphotericin B nephrotoxicity. *Drug Saf* **5**: 94–108.

Shao LC, Sheng CQ, Zhang WN. 2007. Recent advances in the study of antifungal lead compounds with new chemical scaffolds. *Acta Pharmacol Sin* **42**: 1129–1136.

Shin S, Lim S. 2004. Antifungal effects of herbal essential oils alone and in combination with ketoconazole against Trichophyton spp. *J Appl Microbiol* **97**: 1289–1296.

Uno J, Shigematsu ML, Arai T. 1983. Novel synergism of two antifungal agents, copiamycin and imidazole. *Antimicrob Agents Chemother* **24**: 552–559.

US Food and Drug Administration. 2001.Guidance for Industry – Bioanalytical Method Validation. Washington, DC.

Zhang L, Yan K, Zhang Y *et al*. 2007. High-throughput synergy screening identifies microbial metabolites as combination agents for the treatment of fungal infections. *Proc Natl Acad Sci USA* **104**: 4606–4611.